The Astrophysical Journal Letters, 957:L10 (7pp), 2023 November 1 https://doi.org/10.3847/2041-8213/acff62

First Metis Detection of the Helium D_3 Line Polarization in a Large Eruptive Prominence

Petr Heinzel[1,2], Sonja Jejčič[1,3,4], Jiří Štěpán[1], Roberto Susino[5], Vincenzo Andretta[6], Giuliana Russano[6], Silvano Fineschi[5], Marco Romoli[7,8], Alessandro Bemporad[5], Arkadiusz Berlicki[1,2], Aleksandr Burtovoi[8], Vania Da Deppo[9], Yara De Leo[10], Catia Grimani[11], Giovanna Jerse[12], Federico Landini[5], Giampiero Naletto[13], Gianalfredo Nicolini[5], Maurizio Pancrazzi[5], Tanausú del Pino Alemán[14,15], Clementina Sasso[16], Daniele Spadaro[17], Marco Stangalini[18], Daniele Telloni[5], Luca Teriaca[10], Michela Uslenghi[19], and Andrés Vicente Arévalo[14,15]

[1] Astronomical Institute, The Czech Academy of Sciences, 25165 Ondřejov, Czech Republic; pheinzel@asu.cas.cz
[2] Center of Excellence—Solar and Stellar Activity, University of Wroclaw, Kopernika 11, 51 622 Wroclaw, Poland
[3] Faculty of Education, University of Ljubljana, Kardeljeva ploščad 16, 1000 Ljubljana, Slovenia
[4] Faculty of Mathematics and Physics, University of Ljubljana, Jadranska 19, 1000 Ljubljana, Slovenia
[5] Instituto Nationale di Astrofisica (INAF)—Turin Astrophysical Observatory, Via Osservatorio 20, I-10025 Pino Torinese, TO, Italy
[6] Instituto Nationale di Astrofisica (INAF)—Osservatorio Astronomico di Capodimonte, Salita Moiariello 16, I-80 131 Napoli, Italy
[7] University of Firenze, Departmen of Physics and Astronomy, ViaGiovanni Sansone 1, I-50019 Sesto Fiorentino, Firenze, Italy
[8] Instituto Nationale di Astrofisica (INAF)—Osservatorio Astrofisico di Arcetri, Firenze, Italy
[9] National Research Council and Institute for Photonics and Nanotechnologies (CNR—IFN), Via Trasea 7, 35131, Padova, Italy
[10] Max Planck Institute for Solar System Research, Justus-von-Liebig-Weg 3, D-37077, Göttingen, Germany
[11] Dipartimento di Scienze Pure e Applicate, Universitá di Urbino National Institute for Nuclear Physics (INFN), Via Sant'Andrea, 34, 61029 Urbino, Italy
[12] Instituto Nationale di Astrofisica (INAF)—Osservatorio Astronomico di Trieste, 34143, Via Pasquale Besenghi, 17, 34144 Trieste, Italy
[13] Dipartimento di Fisica e Astronomia, Universitá di Padova,Via Francesco Marzolo, 8, 35121 Padova, Italy
[14] Instituto de Astrofísica de Canarias, E-38205 La Laguna, Tenerife, Spain
[15] Departamento de Astrofísica, Universidad de La Laguna, E-38206 La Laguna, Tenerife, Spain
[16] Instituto Nationale di Astrofisica (INAF)—Astronomical Observatory of Capodimonte, Salita Moiariello 16, I-80 131 Naples, Italy
[17] Instituto Nationale di Astrofisica (INAF)—Osservatorio Astrofisico di Catania, Via S. Sofia, 78, 95123 Catania, Italy
[18] Agenzia Spaziale Italiana (ASI), Roma, Via del Politecnico, 00133 Roma, Italy
[19] Instituto Nationale di Astrofisica and Istituto di Astrofisica Spaziale e Fisica (INAF—IASF) Milano, Via Alfonso Corti, 20133 Milano, Italy
Received 2023 August 19; revised 2023 October 2; accepted 2023 October 2; published 2023 October 30

Abstract

Metis on board Solar Orbiter is the space coronagraph developed by an Italian–German–Czech consortium. It is capable of observing solar corona and various coronal structures in the visible-light (VL) and UV (hydrogen Lyα) channels simultaneously for the first time. Here we present observations of a large eruptive prominence on 2021 April 25–26, in the VL, taken during the mission cruise phase, and demonstrate that apart from the broadband continuum emission, which is due to the Thomson scattering on prominence electrons, we detect a significant radiation in the neutral-helium D_3 line (587.6 nm), which lies within the Metis VL passband. We show how the prominence looks like in Stokes I, Q, and U. We consider two extreme cases of the prominence magnetic field, and we separate the Stokes I and Q signals pertinent to Thomson scattering and to the D_3 line. The degree of linear polarization of the D_3 line (both Q and U) indicates the presence of the prominence magnetic field; hence Metis can serve as a magnetograph for eruptive prominences located high in the corona.

Unified Astronomy Thesaurus concepts: Solar prominences (1519); Coronagraphic imaging (313); Solar corona (1483); Solar coronal mass ejections (310)

1. Introduction

Solar Orbiter, a mission toward the Sun, was launched in 2020 February, and its principal goal is to improve our understanding of the complexity of the solar activity and its effects on the heliosphere. Among 10 on board instruments, Metis is the space coronagraph dedicated to study the coronal activity and properties of the solar wind (Antonucci et al. 2020; Fineschi et al. 2020). It represents a new generation of externally occulted coronagraphs with a compact design based on special annulus-type main mirrors. Metis has two spectral channels, the visible-light (VL) channel and the ultraviolet (UV) one. The VL channel with passband 580–640 nm is similar to those on other space coronagraphs like SOHO/LASCO-C2 or STEREO-A/COR1 and is aimed at the study of coronal structures and their dynamics in the VL predominantly produced by the Thomson scattering on free electrons. This channel provides three Stokes parameters, i.e., the intensity I and two Stokes parameters of linear polarization Q and U. The UV channel detects the integral emission of the hydrogen Lyα line. Both channels can detect well the time evolution of studied processes, namely the fast-evolving coronal mass ejections (CMEs) and eruptive prominences. A combination of VL and UV images can provide temperature and density diagnostics of the coronal plasmas (e.g., Susino & Bemporad 2016). Lyα emission from the core of a CME was recently studied by Heinzel et al. (2016), Jejčič et al. (2017), Susino et al. (2018), and references therein using SOHO/UVCS spectra and VL data from SOHO/LASCO-C2. Recently Floyd & Lamy (2019) presented in-depth analysis of several eruptive events as also observed by the SOHO/LASCO-C2 coronagraph with the orange VL filter. They analyzed the linear polarization and found several cases of very low-degree polarization brightness, which indicated possible effects of the helium D_3 line (neutral helium line at 587.6 nm), which is

present within the orange filter. The authors suggested that a lowering of the polarization degree could be caused by the Hanle effect, i.e., depolarization of the D_3 emission in the presence of a magnetic field. Subsequently, motivated by the fact that also the Metis VL channel contains the D_3 line in its passband, Heinzel et al. (2020) made a theoretical synthesis of the expected Metis VL signal composed of the Thomson scattering and D_3 components. They also predicted the degree of linear polarization U/I which can be nonzero only in the presence of a substantial D_3 emission from relatively cool eruptive prominences. In this paper we use, for the first time, a set of all three Stokes parameters I, Q, and U detected by Metis in an eruptive prominence and demonstrate the signatures of the D_3 line emission and polarization. Note that the D_3 line polarization was extensively studied in the past (see a review by López Ariste 2015) but only in the case of low-lying quiescent prominences. Metis thus can provide the first insight into the structure of the magnetic field of eruptive events propagating through the corona at large altitudes.

2. Prominence Observations and Data Reduction

The Metis coronagraph on board Solar Orbiter provides images of the solar corona in the broadband VL channel between 580 and 640 nm in total and polarized brightness and in polarization angle encoded in the Stokes parameters I, Q, and U. On 2021 April 25–26, the Metis coronagraph observed the eruptive prominence moving in the core of a CME between 22 UT on April 25 and 6 UT and April 26. During the observations, the Solar Orbiter was at a distance of 0.879 au from the Sun. At this distance, the Metis field of view was between 5.3 and 11.2 solar radii. The VL images were acquired with an exposure time of 450 s, a cadence of 1830 s, and a binning factor of 4 in both axes of the CCD camera, corresponding to a spatial scale of $40''\,\mathrm{pixel}^{-1}$ ($\sim$25,000 km pixel^{-1} on the plane of sky, PoS). We used the VL polarized level-2 data processed by the Metis pipeline, in particular to analyze the Stokes parameters I, Q, and U. The reference system for the Stokes parameters is redefined locally in the coronal image, bin by bin, aligning the negative Q parameter along the radial direction and the positive Q parameter along a direction perpendicular to the radial direction from the Sun's center (i.e., parallel to the nearest solar limb), in such a way that the pure Thomson scattering of uniform disk solar radiation that dominates the broadband VL brightness will have a Stokes vector with positive Q and null U parameters. For the analysis, we selected an eruptive prominence imaged at 01:05 UT on 2021 April 26. Note that this is the starting time of the exposure according to the fits file header. Figure 1 shows the position of Solar Orbiter on 2021 April 26 at 00:00 UT with respect to Earth together with STEREO-A, SOHO, and Parker Solar Probe in the Carrington coordinate system (Gieseler et al. 2023). The position of the eruptive prominence is also marked by a black arrow determined by the triangulation method (Russano et al. 2023).

3. Spatial Behavior of the VL Polarization

In Figure 2 we see a snapshot of the eruptive prominence observed at 01:05 UT, together with the pre-event corona. In the upper panel, the intensity I seems to be dominated by the F-corona emission, while the prominence itself is rather weak. The Stokes Q image shows clearly that both the prominence as

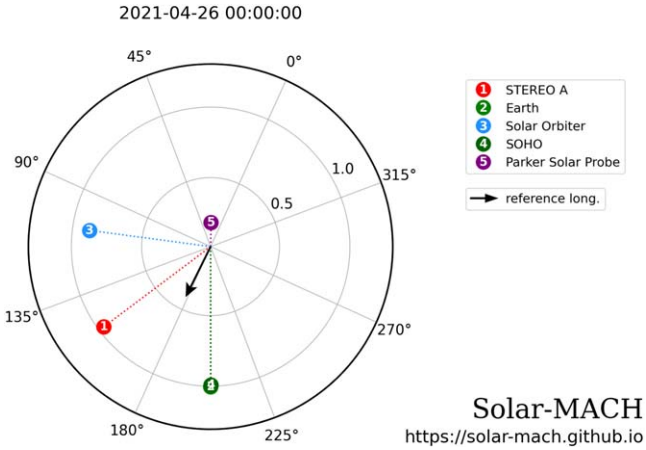

Figure 1. Position of the Solar Orbiter during prominence observations.

well as some streamer-like features are linearly polarized. In the prominence, it can in principle be due to Thomson scattering, but we will demonstrate the presence of a significant effect of the helium D_3 line. However, most interesting is the lower panel where we clearly see a non-negligible Stokes U signal, which we further assign to the presence of the D_3 line emission within the prominence. In order to get a pure prominence emission, we subtracted the background coronal signal. To do this, we made various experiments, and finally, we decided to use a pre-event image shown in the middle panel. Note that all images have been first processed to level-2 data and radiometrically calibrated in mean solar brightness (MSB) units ($1\ \mathrm{MSB} = 1.52 \times 10^9\ \mathrm{erg\ s^{-1}\ cm^{-2}\ sr^{-1}}$). After the subtraction, we got images in the lower panel where the eruptive prominence is clearly visible although the Stokes U image is somewhat noisier. As the next step we followed a spiral-like shape of the prominence threads and marked the brightest pixels when making perpendicular cuts through the threads. Such a chain of the brightest pixels is shown in Figure 3 for "northern" and "southern" threads. For these pixels we constructed plots of Stokes parameters (in MSB units) depending on their distance in the PoS from the Sun's center, d (see Figure 4). In general we see a good correlation between I, Q, and U, but again Stokes U is noisier. Finally, in Figure 5 we plot the characteristic ratios Q/I and U/I, which we will discuss in the next sections.

We admit that at this moment we are not certain about the level of uncertainties of the data, which complicates the quantitative analysis. The subtraction process might have introduced a significant error into the data. Since the U/I signal is systematically positive across the studied region, it suggests that it is either a real signal above the noise level or a systematic error in the data. In the former case, the problem arises because no such strong U/I signal can be produced by the D_3 line in the considered geometry. In the latter case, we have to admit that both Q/I and U/I may be affected by an unknown systematic error or certain calibration issues, namely, unrealistically high U/I. Especially close to the occulter, the vignetting may produce some spurious signal; see the Metis calibration paper by Liberatore et al. (2023). In addition, we note that there is a non-negligible U/I signal already in the pre-event data, which is difficult to explain without considering a systematic error in the data processing. For these reasons, we emphasize that our data need to be taken with caution.

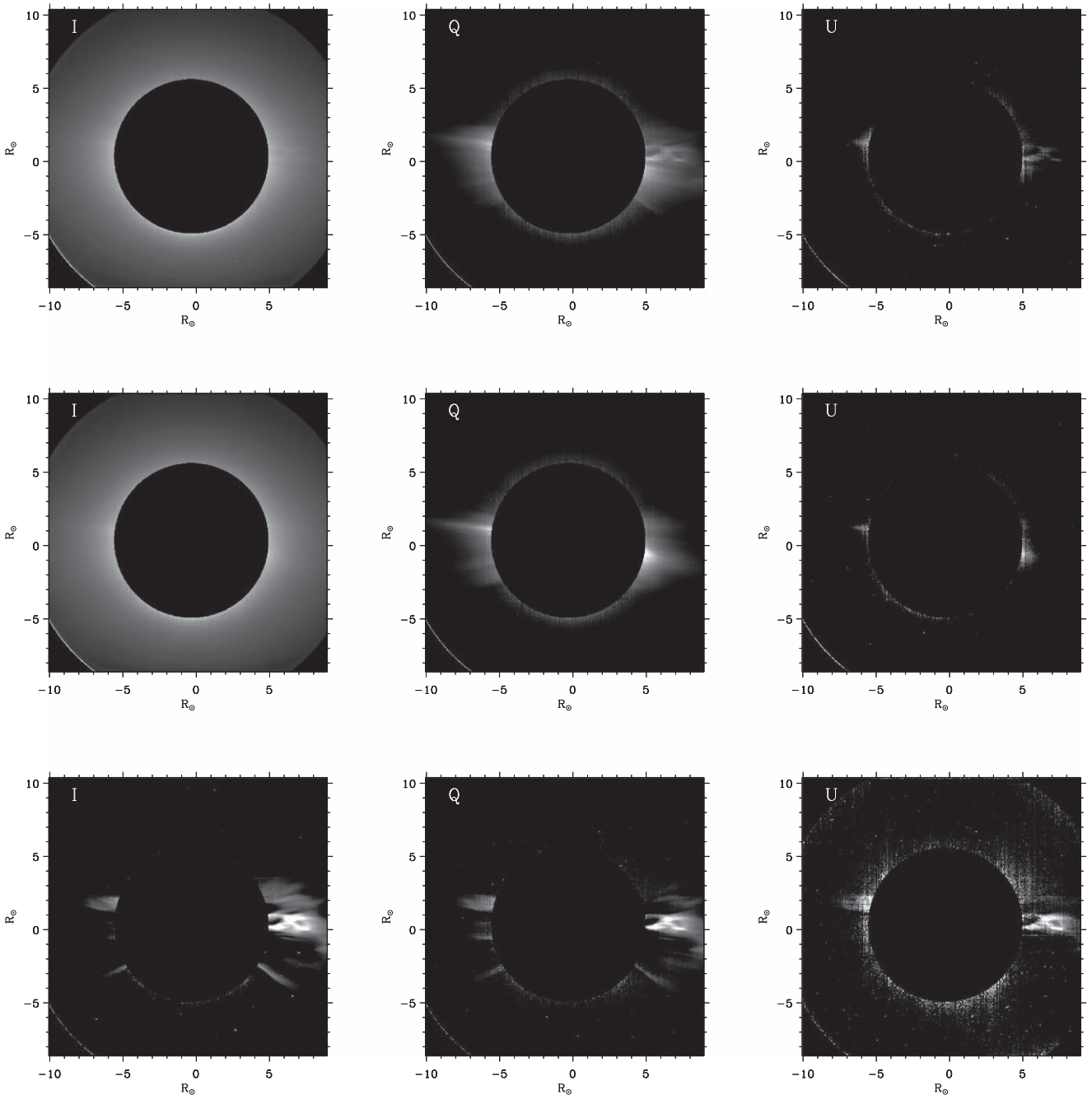

Figure 2. Eruptive prominence as detected by Metis VL channel on 2021 April 26 at 01:05 UT (upper panels—Stokes *I*, *Q*, *U*); on middle panels, Stokes *I*, *Q*, *U* are shown on 2021 April 25 at 15:05 UT as the pre-event image. Lower panels show the prominence observation with pre-event corona subtracted. Note that three Stokes images are shown with different contrasts in order to enhance structures of interest, but they have been obtained within the same field of view.

4. Formation of VL Polarized Radiation

We have used methods of Bayesian inference to derive the densities and the magnetic field vector from the Stokes parameters *I*, *Q*, and *U*. However, given the uncertain level of noise and possible presence of a systematic error in Stokes *U* that may also be affected by subtraction of the pre-event data, our results were inconclusive. Therefore, we limit our quantitative analysis to a much less ambitious calculation of just two limiting cases providing us with maximum and minimum densities and only using the values of Stokes *I* and *Q*. This approach should be understood as just an order-of-magnitude estimation, and a more detailed analysis shall be done in the future. Below we describe our calculation of the densities using the Stokes *I* and *Q* parameters.

The total observed intensity and Stokes *Q* emitted by a slab of geometrical thickness *d* can be decomposed as

$$I = I_{\rm T} + I_{\rm D} = n_{\rm e} d\epsilon_I^{\rm T} + n_{\rm He} d\epsilon_I^{\rm D} = n_{\rm e} d(\epsilon_I^{\rm T} + \gamma\epsilon_I^{\rm D}), \quad (1)$$

$$Q = Q_{\rm T} + Q_{\rm D} = n_{\rm e} d\epsilon_Q^{\rm T} + n_{\rm He} d\epsilon_Q^{\rm D} = n_{\rm e} d(\epsilon_Q^{\rm T} + \gamma\epsilon_Q^{\rm D}), \quad (2)$$

where $\gamma = n_{\rm He}/n_{\rm e}$ is the ratio of the orthohelium and electron density and where the indices T and D denote the Thomson and D_3 contributions, respectively. These equations can be solved

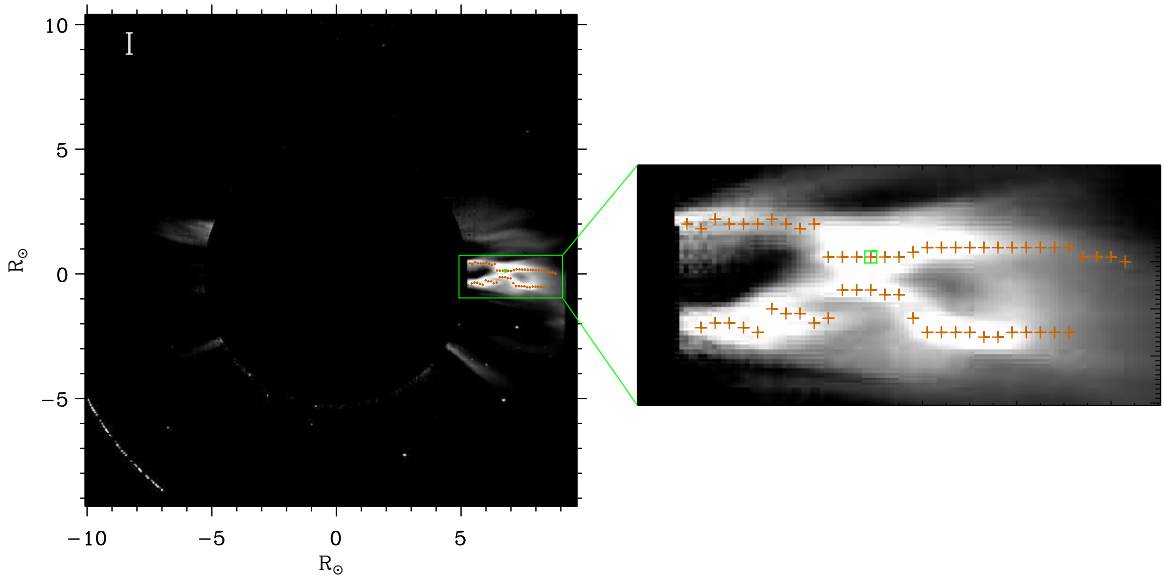

Figure 3. Selected brightest pixels in Stokes I within two prominence arms, which we denote "northern" and "southern." In the zoomed-in panel, the most intense northern pixel, studied in detail, is marked by a green square.

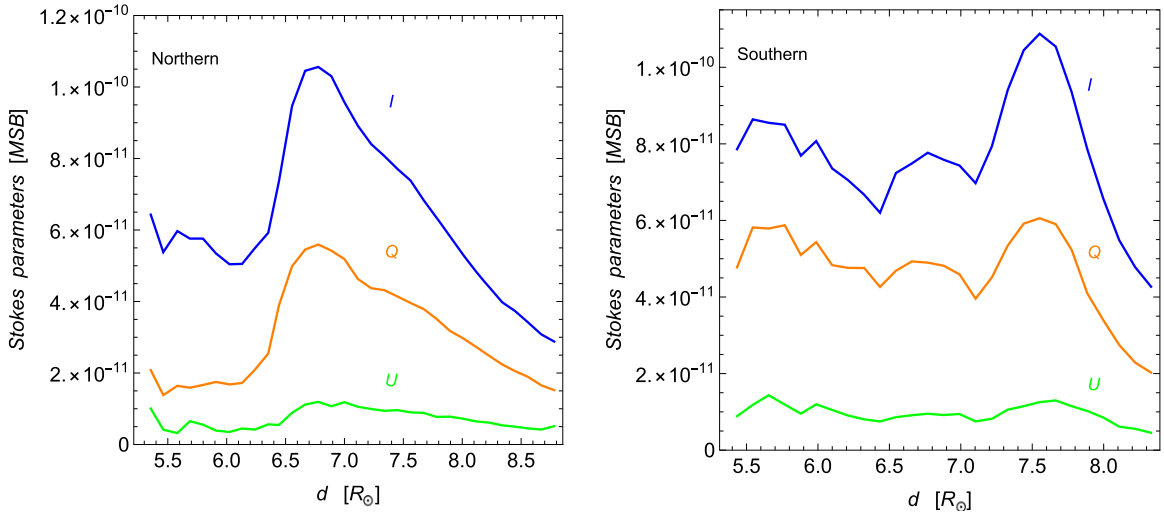

Figure 4. Height variations of I, Q, and U through the brightest pixels shown by orange crosses in Figure 3.

for the unknown quantities γ and $n_e d$:

$$\gamma = \frac{\epsilon_Q^{\mathrm{T}} - \frac{Q}{I}\epsilon_I^{\mathrm{T}}}{\frac{Q}{I}\epsilon_I^{\mathrm{D}} - \epsilon_Q^{\mathrm{D}}}, \tag{3}$$

$$n_e d = \frac{I}{\epsilon_I^{\mathrm{T}} + \gamma\epsilon_I^{\mathrm{D}}}. \tag{4}$$

The quantities ϵ_i^j are determined by the intensity and anisotropy of the solar incident radiation and by the magnetic field. If θ is the angle between the local solar vertical and the line of sight, the Thomson scattering contributions are given by the following expressions:

$$\epsilon_I^{\mathrm{T}} = \sigma_{\mathrm{T}} \int d\nu\ \phi(\nu) J_0^0(\nu) \left[1 + \frac{1}{2\sqrt{2}}(3\cos^2\theta - 1)\frac{J_0^2(\nu)}{J_0^0(\nu)}\right], \tag{5}$$

$$\epsilon_Q^{\mathrm{T}} = \sigma_{\mathrm{T}} \int d\nu\ \phi(\nu) \frac{3}{2\sqrt{2}}(1 - \cos^2\theta) J_0^2(\nu), \tag{6}$$

where $\sigma_{\mathrm{T}} = 6.65 \times 10^{-25}\,\mathrm{cm}^2$ is the Thomson scattering cross section and $\phi(\nu)$ is the Metis VL passband profile. The radiation-field intensity and anisotropy at a given location in the corona can be quantified by the two radiation-field tensor components J_0^0 and J_0^2 (Landi Degl'Innocenti & Landolfi 2004).

The D_3 contributions, ϵ_I^{D} and ϵ_Q^{D}, are frequency-integrated emission coefficients given by Equations 7.47(b) and 7.47(e) of Landi Degl'Innocenti & Landolfi (2004), normalized with respect to the number density of the atoms. In contrast to the Thomson scattering contribution, these coefficients depend not only on $J_0^K(\nu)$ but also on the local magnetic field vector via the Hanle effect.

In order to derive the electron column density and the orthohelium-to-electron density, we consider two extreme examples of the magnetic field configuration: (i) zero magnetic

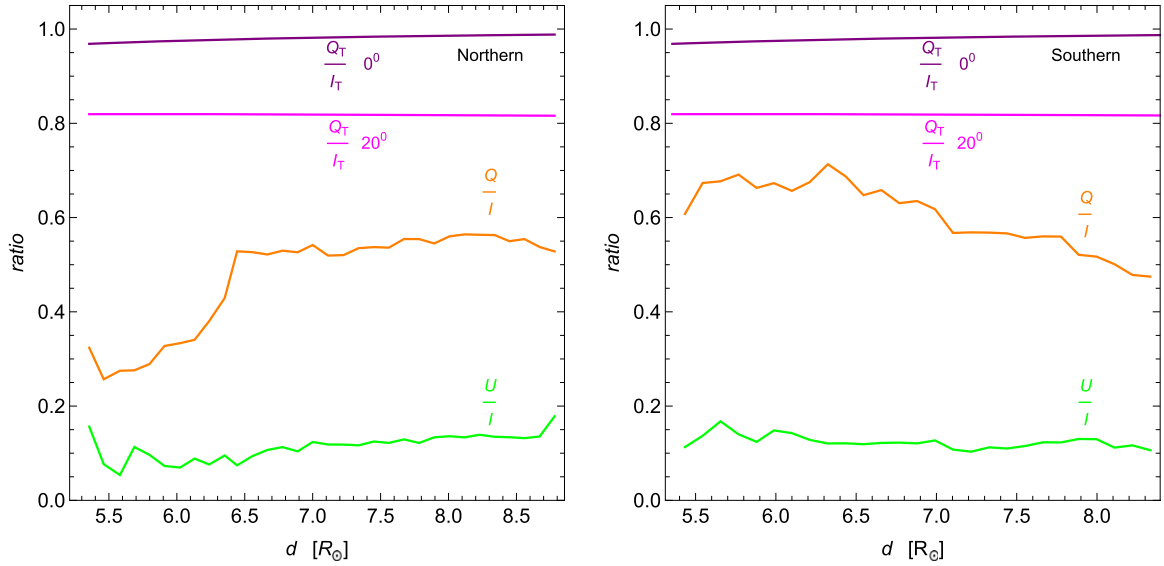

Figure 5. Plot of the observed ratios Q/I and U/I. Theoretical ratios due to Thomson scattering are also shown for two deviations from the Metis PoS.

Table 1
Stokes Parameters in the Brightest Northern Pixel (in MSB Units)

	I	Q	U
Total	8.136(−10)	8.999(−11)	2.125(−11)
Pre-event	7.080(−10)	3.405(−11)	9.323(−12)
Corrected	1.056(−10)	5.595(−11)	1.193(−11)

Note. 8.136(−10) corresponds to 8.136×10^{-10}.

field ($B = 0$ G); (ii) magnetic field much stronger than the Hanle-effect critical magnetic field B_H (i.e., the D_3 line is in the Hanle-effect saturation regime; see, e.g., Table 1 of Asensio Ramos et al. 2008) parallel to the LoS. In the former case, the contribution of the D_3 line to Stokes Q is maximized, while in the latter case the polarization emission due to ϵ_Q^D is zero, and the line only contributes to the total intensity via ϵ_I^D.

5. Helium D_3 Line Emission

For the following analysis it is quite important to know the position of the prominence with respect to the PoS of Metis at the time of observations. This eruptive prominence was also observed in the UV channel of Metis, and the UV data are reported by Russano et al. (2023). The authors determined the angle by which the prominence deviates from the Metis PoS, and they provided the value 19°.3 using the triangulation technique (see their paper for details). As it is well known, at sufficient heights above the solar surface, the maximum linear polarization due to Thomson scattering is obtained when the prominence is located exactly within the PoS. The polarization ratio also increases with height due to increasing anisotropy of the incident limb-darkened photospheric radiation (see Figure 5). The observed Q/I is well below that for pure Thomson scattering at 19°.3, and also its height variations are indicative of another emission mechanism.

Further on we will focus on one specific position in the northern part of the prominence where all three Stokes values reach their maximum. This position is marked by a green square in the right panel of Figure 3. The distance from the disk center is 6.78 $R_\odot$. Measured Stokes intensities are summarized in Table 1 in MSB units. Table 2 then presents the results of our inference. Note that for both T and D components the polarization ratios are simply given by the ratios of the respective emission coefficients. The electron column densities in Table 2 look quite reasonable; they are comparable to values inferred by Heinzel et al. (2016) from UVCS observations in hydrogen Lyman lines, and they also agree well with those obtained for this prominence by Russano et al. (2023). The mean electron density will then depend on the expected geometrical effective thickness d, which is the line-of-sight path occupied by the prominence plasma (e.g., Susino et al. 2018). For an ad hoc value of $d = 10^5$ km, we get the electron densities (i) 1.87×10^6 cm^{-3} and (ii) 2.43×10^6 cm^{-3}. The variation with height of the electron column density and parameter γ is shown in Figure 6.

Considering only the Thomson scattering, we get the theoretical value $Q_T/I_T = 0.83$ for the angle 19°.3. In Table 1 we present the calibrated values of Stokes parameters ("corrected" are those with subtracted pre-event values). From them we get $Q_{cor}/I_{cor} = 0.53$ and $U_{cor}/I_{cor} = 0.11$. We see that the observed ratio Q_{cor}/I_{cor} is much smaller than the theoretical one for pure Thomson scattering, and this applies also to the majority of other pixels (see Figure 5). This clearly indicates the presence of helium D_3 line emission within the Metis VL channel, as theoretically predicted by Heinzel et al. (2020). Note that the pre-event $I = 7.08 \times 10^{-10}$ (in MSB units) at this particular pixel, similar to other coronal pixels, is consistent with the value usually reported in the literature for the F-corona, which is expected to dominate the quiet coronal VL emission at such large heights. Given the limited knowledge of the data uncertainties, we only provide the values in Tables 1 and 2 without error bars.

Linear polarization of the D_3 radiation is due to the scattering of anisotropic photospheric radiation, the so-called resonant scattering polarization. The anisotropy of the incident radiation is due to the prominence location high in the corona and also due to the center-to-limb variation of the photospheric continuum around the D_3 line. This scattering polarization signal is then added to that due to Thomson scattering. From the results presented in Table 2 we can draw the following conclusions. The relative contribution of D_3 emission to total

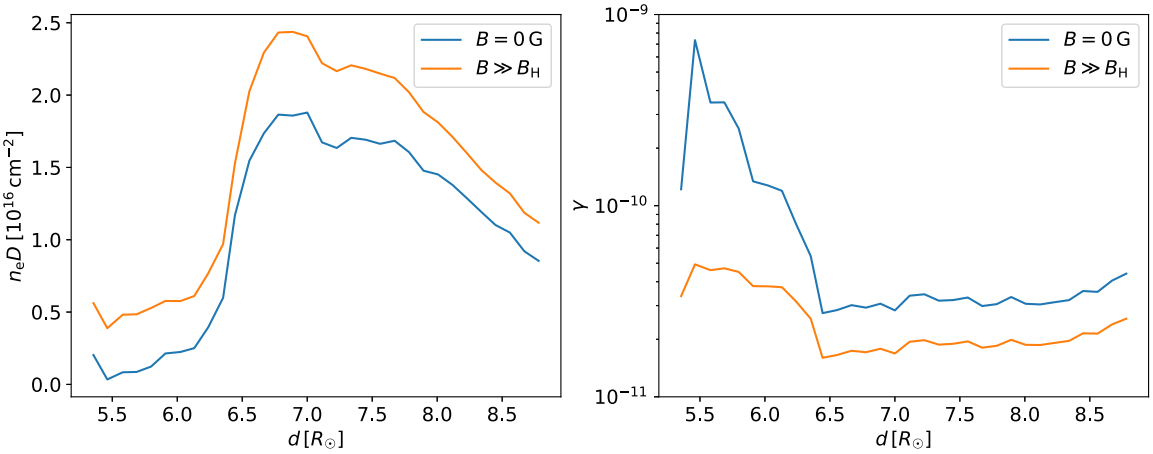

Figure 6. Electron column densities (per square centimeter) and the ratio of orthohelium density to electron density for two extreme solutions within the northern prominence arm.

Table 2
Results of Inference for the Selected Pixel[a]

B	$n_e d$	γ	ϵ_I^T	ϵ_Q^T	ϵ_I^D	ϵ_Q^D	I_T	Q_T	I_D	Q_D
$B = 0$	1.87(+16)	2.93(−11)	2.77(−27)	2.30(−27)	9.87(−17)	2.39(−17)	5.18(−11)	4.30(−11)	5.41(−11)	1.31(−11)
$B \gg B_H$	2.43(+16)	1.71(−11)	2.77(−27)	2.30(−27)	9.16(−17)	0	6.73(−11)	5.59(−11)	3.81(−11)	0

Note.
[a] We point out that the integrated emissivity of the D_3 line, ϵ_I^D, can also be modified by the magnetic field. This is due to the fact that emissivity of the Stokes I parameter is not only affected by atomic level population but also by the level of polarization induced by anisotropic illumination from the solar disk. As the atomic level polarization is modified by the Hanle effect, ϵ_I^D is modified accordingly (see, e.g., Landi Degl'Innocenti & Landolfi 2004).

intensity integrated over the Metis VL passband is (i) 0.51 and (ii) 0.36, which is quite significant. The ratio I_D/I_T is (i) 1.04 and (ii) 0.57. The polarization degree of the helium line Q_D/I_D amounts to 0.24 in case of (i) but goes to zero for large B as expected. In low-lying quiescent prominences, this polarization degree was detected up to a few percent. In the presence of a magnetic field, the line polarization is lowered, and the polarization plane is rotated due to the Hanle effect. In such case, a nonzero U_D appears.

6. Conclusions and Future Prospects

Our principal focus was to clearly demonstrate the importance of the helium D_3 line emission from the observed eruptive prominence within the Metis VL passband. For this particular event we found that the relative contribution of the D_3 line emission to total intensity I_D/I can reach up to 50%, which is quite important and indicates the presence of a large amount of cool prominence material very high in the corona. This also leads to a significant lowering of the polarization degree Q/I, which, taking into account the prominence location with respect to PoS, cannot be explained by the Thomson scattering on prominence electrons. Similar lowering was also detected in several eruptive prominences by Floyd & Lamy (2019) using the SOHO/LASCO-C2 observations (with the orange filter also containing the D_3 line) and by Mierla et al. (2011) using STEREO observations where the VL channel contained the hydrogen Hα line. The presence of Hα was also analyzed using the LASCO red filter by Dolei et al. (2014). With Metis we now confirm some previous LASCO results, which concern the unexpectedly low polarization degree and go further in deriving the intensity and polarization of the helium D_3 line. The presence of the non-negligible D_3 emission within the Metis VL channel offers a unique possibility to infer the characteristics of the erupting prominence magnetic field as proposed in Heinzel et al. (2020). A lowering of D_3 polarization due to the Hanle effect is representative of the magnetic field, and a nonzero U_D must also result from its presence. Using the values of I, Q, and U as discussed in the previous sections, we have tried to infer the magnetic field using techniques of Bayesian inference, accounting also for the observed Stokes U. However, we were unable to reproduce rather high values of U/I, which reach 10%–20%. We also analyzed another erupting prominence (2021 October 2) and found a similar, rather large U/I. The uncertainties in the absolute calibration of the Stokes parameters should not be very large, around 10%–15%. So the question remains why the polarization degree U/I is so high. At the moment, we do not see any good physical reason for that, but we cannot exclude that some systematic enhancement exists. Note, however, that U/Q is typically around 20%, and this should not change significantly our results based on the ratio Q/I even if we would assume some kind of coupling between Q and U signals. In fact we see in Figure 2, the second row, that the pre-event streamers well visible in Stokes Q are also recognized in U with a similar shape. This is probably due to calibration issues close to the occulter as we also mention elsewhere. We plan to check carefully the whole procedure of data reduction and calibration but also the reliability of our inference approach in case of this particular problem. Metis has already observed several eruptive events like the one shown here, and several of them were also detected in the UV channel in the hydrogen Lyα line. The latter, combined with the VL data, can provide the density and temperature diagnostics of the prominence. Putting all this

together and adding the Stokes U into inversions inferences will be the subject of our future analysis. A realistic determination of the magnetic field will be possible when a bright prominence is observed at the closest approach of the Solar Orbiter to the Sun.

Acknowledgments

Solar Orbiter is the ESA mission toward the Sun launched by NASA on 2020 February 10. Metis is its payload coronagraph developed by the Italian–German–Czech consortium, with funding from the Italian Space Agency (ASI), under contracts to the National Institute of Astrophysics (INAF) and industrial partners. Metis was built with hardware contributions from Germany (Bundesministerium für Wirtschaft und Energie through DLR), from the Czech Republic (PRODEX) and from ESA. P.H., S.J. and J.Š. acknowledge support from the grant 22-34841S of the Czech Science Foundation and from the project RVO:67985815 of the Astronomical Institute of the Czech Academy of Sciences. This work was also partially supported by the program "Excellence Initiative—Research University" for years 2020–2026 at University of Wroclaw, project no. BPIDUB.4610.96.2021.KG. S.J. acknowledges the support from the Slovenian Research Agency No. P1-0188. Metis team thanks the former PI, Ester Antonucci, for leading the development of Metis until the final delivery to ESA. Partial ionization in solar prominences led by J.-L. Ballester is highly acknowledged. The authors thank the anonymous referee for constructive comments.

Facility: SolO.

ORCID iDs

Petr Heinzel https://orcid.org/0000-0002-5778-2600
Sonja Jejčič https://orcid.org/0000-0001-8489-4037
Jiří Štěpán https://orcid.org/0000-0002-8292-2636
Roberto Susino https://orcid.org/0000-0002-1017-7163
Vincenzo Andretta https://orcid.org/0000-0003-1962-9741
Giuliana Russano https://orcid.org/0000-0002-2433-8706
Marco Romoli https://orcid.org/0000-0001-9921-1198
Alessandro Bemporad https://orcid.org/0000-0001-5796-5653
Arkadiusz Berlicki https://orcid.org/0000-0002-6505-4478
Catia Grimani https://orcid.org/0000-0002-5467-6386
Giampiero Naletto https://orcid.org/0000-0003-2007-3138
Gianalfredo Nicolini https://orcid.org/0000-0002-9459-3841
Maurizio Pancrazzi https://orcid.org/0000-0002-3789-2482
Tanausú del Pino Alemán https://orcid.org/0000-0003-1465-5692
Clementina Sasso https://orcid.org/0000-0002-5163-5837
Daniele Spadaro https://orcid.org/0000-0003-3517-8688
Daniele Telloni https://orcid.org/0000-0002-6710-8142
Luca Teriaca https://orcid.org/0000-0001-7298-2320
Andrés Vicente Arévalo https://orcid.org/0000-0003-3896-836X

References

Antonucci, E., Romoli, M., Andretta, V., et al. 2020, A&A, 642, A10
Asensio Ramos, A., Trujillo Bueno, J., & Landi Degl'Innocenti, E. 2008, ApJ, 683, 542
Dolei, S., Bemporad, A., & Spadaro, D. 2014, A&A, 562, A74
Fineschi, S., Naletto, G., Romoli, M., et al. 2020, ExA, 49, 239
Floyd, O., & Lamy, P. 2019, SoPh, 294, 168
Gieseler, J., Dresing, N., Palmroos, C., et al. 2023, FrASS, 9, 384
Heinzel, P., Susino, R., Jejčič, S., Bemporad, A., & Anzer, U. 2016, A&A, 589, A128
Heinzel, P., Štěpán, J., Bemporad, A., et al. 2020, ApJ, 900, 8
Jejčič, S., Susino, R., Heinzel, P., et al. 2017, A&A, 607, A80
Landi Degl'Innocenti, E., & Landolfi, M. 2004, Polarization in Spectral Lines, Vol. 307 (Dordrecht: Kluwer)
Liberatore, A., Fineschi, S., Casti, M., et al. 2023, A&A, 672, A14
López Ariste, A. 2015, in Solar Prominences, Astrophysics and Space Science Library, ed. J.-C. Vial & O. Engvold (Cham: Springer), 179
Mierla, M., Chifu, I., Inhester, B., Rodriguez, L., & Zhukov, A. 2011, A&A, 530, L1
Russano, G., Andretta, V., De Leo, Y., et al. 2023, A&A, submitted
Susino, R., & Bemporad, A. 2016, ApJ, 830, 58
Susino, R., Bemporad, A., Jejčič, S., & Heinzel, P. 2018, A&A, 617, A21